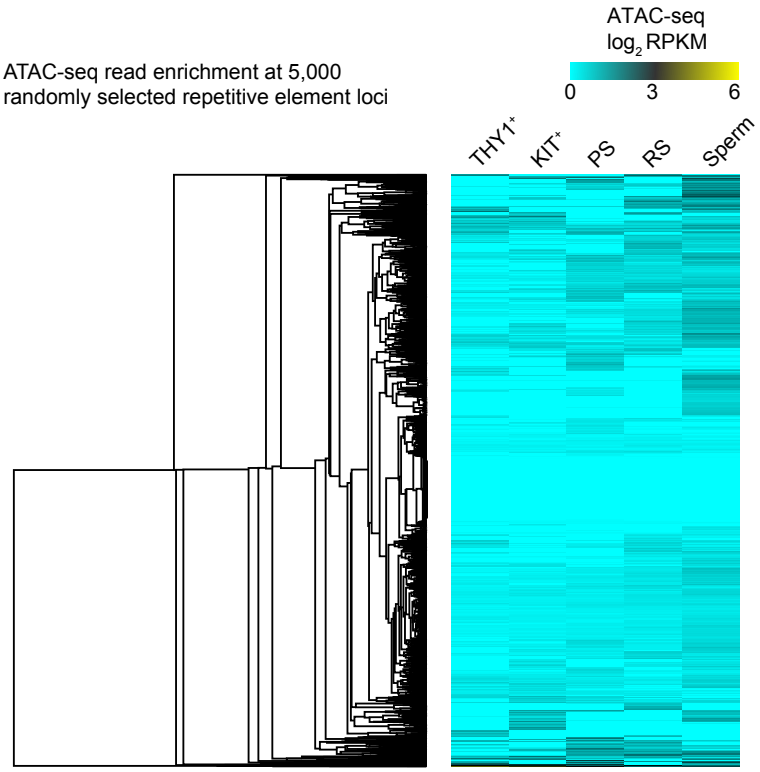

Supplementary Figure 1. ATAC-seq read enrichment at 5,000 randomly selected repetitive element loci.
Heat map depicting RPKM-normalized ATAC-seq reads at 5,000 randomly selected repetitive element loci during spermatogenesis. THY1^{+}, undifferentiated spermatogonia; KIT^{+}, differentiating spermatogonia; PS, pachytene spermatocyte; RS, round spermatids; Sperm: epididymal spermatozoa.

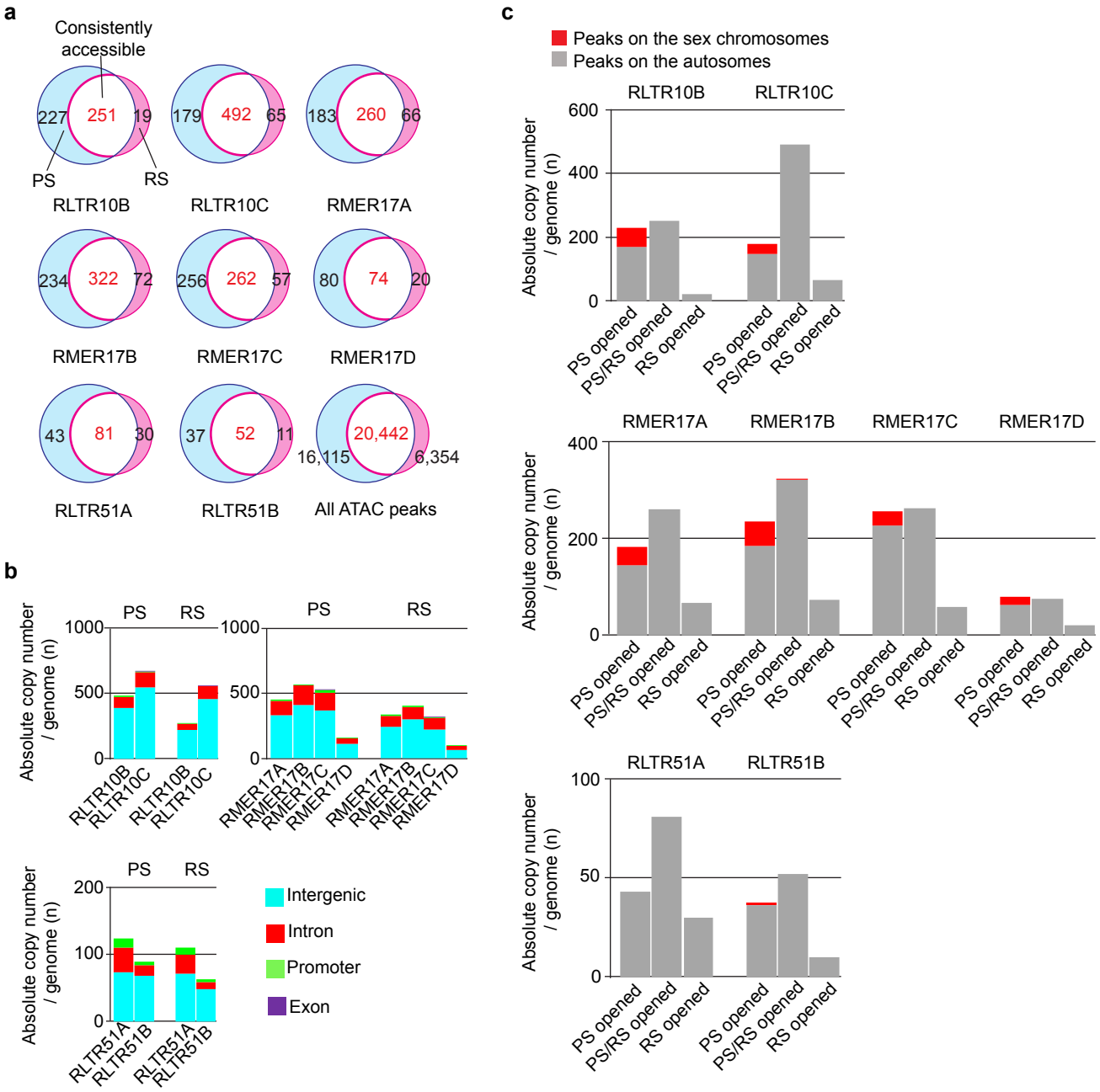

Supplementary Figure 2. Genomic features of accessible ERVKs in late spermatogenesis.
(**a**) Venn diagram showing the overlap of young ERVK loci in accessible chromatin between pachytene spermatocytes (PS; blue) and round spermatids (RS; pink). (**b**) Bar charts depicting genomic distributions of young ERVK loci in accessible chromatin. Distributions are shown with colored bars. (**c**) Bar charts indicating absolute copy numbers on autosomes (gray) and sex chromosomes (red) of young ERVKs.

Supplementary Figure 3. Sequence similarities of young ERVK elements between mouse and rat.
(**a**,**b**) Pairwise alignments of RLTR10B (**a**) and RMER17A (**b**) entire consensus sequences between mouse and rat.

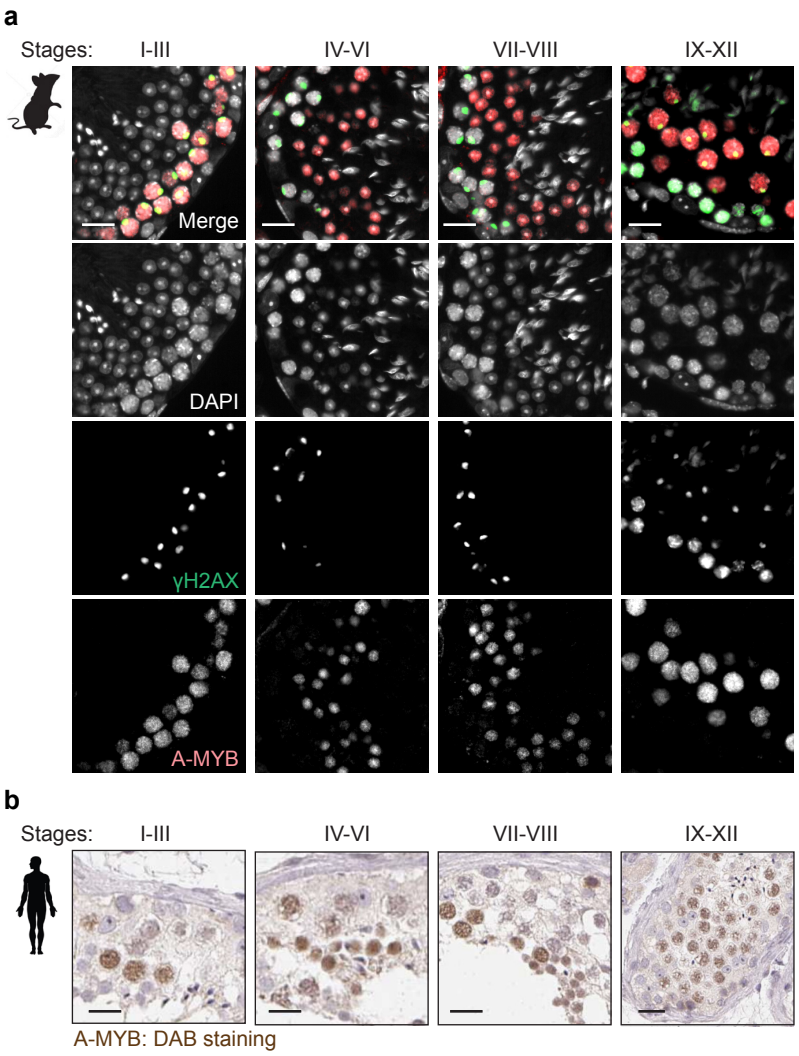

Supplementary Figure 4. A-MYB are highly expressed both in mouse and human spermatocytes.
(**a**) Immunofluorescence co-staining of 12-week-old mouse testicular cross sections for A-MYB (red) and γH2AX (green), and counterstaining with DAPI (gray). The Roman numerals indicate cycles of seminiferous epithelium. (**b**) Representative images of immunohistological staining of 29-to-65-year-old human testicular sections for A-MYB (brown) and counterstaining with hematoxylin (adapted from the Human Protein Atlas (www.proteinatlas.org/ENSG00000185697-MYBL1/tissue/testis#img)). Scale Bars: 20 µm.